Short Communication

Early gene expression profiles of anabolic and catabolic molecules in murine bone after a single PTH injection

Tomomaya Yamamoto[a,b#], Haruhi Maruoka[a#], Hiromi Hongo[a], Hirona Yoshino[a], Mai Haraguchi-Kitakamae[a,c], Xuanyu Liu[a], Qi Yao[a], Minqi Li[d], Norio Amizuka[a], Tomoka Hasegawa[a§]

[a] Developmental Biology of Hard Tissue, Graduate School of Dental Medicine, and Faculty of Dental Medicine, Hokkaido University, Japan, [b] Northern Army Medical Unit, Camp Makomanai, Japan Ground Self-Defense Forces, Sapporo, Japan, [c] Division of Craniofacial Development and Tissue Biology, Graduate School of Dentistry, Tohoku University, Sendai, Japan, [d] Center of Osteoporosis and Bone Mineral Research, Department of Bone Metabolism, School of Stomatology, Shandong University, Jinan, China

[#] The authors consider these two investigators as co-authors.

Running title: ***Gene expression after single PTH injection in bone***

[§]Corresponding Author

Tomoka Hasegawa, DDS, Ph.D.
Developmental Biology of Hard Tissue,
Graduate School of Dental Medicine,
Faculty of Dental Medicine, Hokkaido University
Kita 13, Nishi 7, Kita-Ku, Sapporo, Hokkaido, 060-8586, Japan
Tel/fax: +81-11-706-4226
E-mail: hasegawa@den.hokudai.ac.jp

Short Communication

ABSTRACT

The current study examined the gene expression profiles of anabolic and catabolic molecules after a single injection of PTH. No significant changes were observed in the ALP area/TV, TRAP-positive osteoclasts, and static bone histomorphometry parameters. However, during early PTH administration, a sudden and significant decrease in *Runx*2 expression was detected at 1.5 hrs, followed by an immediate elevation, while sclerostin was initially down-regulated but gradually recovered. Meanwhile, *Rankl* level initially increased and then returned to the basal level. The prolonged elevation of anabolic molecules and transient increase in catabolic molecules may contribute to the overall anabolic effect of PTH treatment.

Keywords

Parathyroid hormone (PTH); anabolic effect; Alkaline phosphatase; Runx2; Rankl

1. Introduction

Parathyroid hormone (PTH) stimulates osteoblastic bone formation and resorption, leading to anabolic effects, specifically bone formation based on remodeling [1]. We have previously shown that frequent PTH administration resulted in the formation of thin trabeculae characterized by a thick preosteoblastic cell layer and accelerated bone remodeling [2]. On the other hand, low-frequency PTH administration induced new bone formation through both remodeling-based and modeling-based bone formation. Therefore, the frequency of PTH administration may influence the mechanism of bone formation, suggesting the possibility of different chronological changes in the expression of genes encoding anabolic and catabolic molecules. Additionally, the anabolic effects of PTH have been attributed to the inhibition of sclerostin secreted by osteocytes [3. 4]. Taken together, analyzing the early stages of chronological changes in gene expression related to osteoblastic activities and osteoclastic bone resorption may provide new insights into the anabolic effects of PTH administration.

2. Materials and Methods

2.1. Animal model and tissue preparation

Six-week-old male C57BL/6J mice (n = 42, Japan CLEA, Tokyo, Japan) were used in this study, following the principles for animal care and research use set by Hokkaido University (approval no.: 15-0032). According to our previous study [2], mice were subcutaneously injected with 80 μg/kg/day

of human PTH [1-34] (Sigma-Aldrich Co., LLC., St. Louis, MO) and sacrificed at 0, 1.5, 3, 6, 12, 24, and 48 hrs (n=6 for each time point). Before fixation, mice were anesthetized with an intraperitoneal injection of a combination of anesthetic agents with medetomidine, midazolam, and butorphanol. The blood samples were collected to estimate the concentrations of serum Ca and Pi using enzymatic methods (Oriental Yeast Co., Ltd., Tokyo). The left tibiae were extracted for RT-PCR and real-time PCR analyses. All mice were then perfused with 4% paraformaldehyde diluted in 0.1 M cacodylate buffer (pH 7.4) through the cardiac left ventricle. The right tibiae and femora were decalcified with a 10% ethylene diamine tetraacetic disodium salt solution and dehydrated in increasing ethanol solutions before paraffin embedding or in ascending acetone solutions for epoxy resin embedding (Epon 812, Taab, Berkshire, UK) for transmission electron microscopy (TEM) (Hitachi H-7100, Hitachi Co., Tokyo, Japan), as described previously [5].

2.2 Histochemical detection of ALP and TRAP

As shown previously, dewaxed paraffin sections were examined for tissue nonspecific alkaline phosphatase (ALP) [6]. In brief, dewaxed paraffin sections were incubated with rabbit polyclonal antisera against ALP [7] at a dilution of 1:300 with 1% BSA-PBS for 2-3 hrs at room temperature (RT). Further, the sections were incubated with horseradish-conjugated anti-rabbit IgG (Jackson Immunoresearch Laboratories Inc., West Grove, PA). Tartrate-resistant acid phosphatase (TRAP) was detected as previously described [8]. Briefly, dewaxed paraffin sections were incubated in a solution of 2.5 mg of naphthol AS-BI phosphate (Sigma-Aldrich), 18 mg of red violet LB (Sigma-Aldrich) salt, and 100 mM L (+) tartaric acid (0.76 g, Nacalai Tesque, Inc., Kyoto, Japan) diluted in 30 mL of a 0.1 M sodium acetate buffer (pH 5.0) for 15 min at 37 °C.

2.3. Bone histomorphometry of BV/TV, Tb.N, Tb.Th, and Tb. Sp

Next, we evaluated the static parameters of bone histomorphometry, such as bone volume/tissue volume (BV/TV %), trabecular number (Tb.N /mm), trabecular thickness (Tb.Th mcm), and trabecular separation (TB. Sp mcm). ALP-immunoreactive osteoblastic area/tissue volume (%), the numbers of TRAP-positive osteoclasts/bone surface (N/μm), the ratio of sclerostin-immunopositive osteocytes/all osteocytes were measured according to our previous study [2]. A 1.3 mm x 2.0 mm region of interest (ROI) located 1.5 mm below the growth plate of the tibial metaphysis was selected for determining the static parameters of bone histomorphometry, ALP-reactive area, the numbers of TRAP-positive cells, and the numbers of sclerostin-reactive cells.

2.4. Gene expression analyses by RT-PCR and real-time PCR

The left tibiae were homogenized in 10 mL of TRIzol reagent (Life Technologies Co., Carlsbad, CA) per 1 g tissue to extract total RNAs. Using the extracted RNAs, first-strand cDNA was synthesized from 2 μg of total RNA using the SuperScript VILO cDNA Synthesis Kit (Life Technologies). The primer sequences used for RT-PCR were as follows: mouse *Gapdh* forward: TGTCTTCACCACCATG GAGAAGG, reverse: GTGGATGCAGGGATGATGTT CTG; mouse *Runx2* forward: GCCCTCTCCAAGACATATA, reverse: CCATGATCACGTCGATATCC; mouse *Rankl* forward: TCGCTCTGTTCCTGTACTTTCG, reverse: GTAGGTACGCTTCCCGATGT; mouse *Osteoprotegerin (Opg)* forward: TGGAGATCGAATTCTGCTTG, reverse: TCAAGTGCTTGAGGGCATAC. PCR was performed using a thermal cycler (GeneAmp PCR System 2700; Applied Biosystems, Foster City, CA). RT-PCR products were electrophoresed on a 2% agarose gel, stained with ethidium bromide, and detected using E-Gel Imager (Life Technologies). Real-time PCR assays were performed using Taqman probes (Applied Biosystems) for evaluating the expressions of *Runx2* (Mm00501584_m1), *Sost* (Mm00470479_m1), *Rankl* (Mm00441906_m1), and *Opg* (Mm00435454_m1). The gene expressions were detected using the StepOne Real-Time PCR System (Applied Biosystems) and normalized to *Gapdh* (Mm99999915_g1) expression using the 2ΔΔCt method.

2.5. Statistical analysis

All values are presented as mean ± standard error. All statistical analyses were conducted using BellCurve for Excel version 2.00 (Social Survey Research Information Co., Ltd., Tokyo, Japan) and analyzed for statistical significance by one-way ANOVA followed by Dunnett's test. A P-value <0.05 was considered significant.

3. Results and Discussion

During the 48 hrs following a single hPTH administration [1-34], there were no significant differences observed in bone histology **(Fig. 1A-N)** and the static parameters of bone histomorphometry such as BV/TV, Tb.Th., Tb.N., and Tb.Sp **(Fig. 1O-R)**. Therefore, a single PTH injection does not appear to be enough to affect bone histology. Serum concentrations of Ca and Pi were also maintained after a single injection of PTH **(Fig. 1S, T)**. There was a slight tendency for a rapid and transient increase in serum Ca, although it was not statistically significant, suggesting that renal regulation of serum Ca concentration was predominantly maintained [8].

Regarding anabolic indices, the expression of *Runx2* transiently decreased at 1.5 hrs after PTH administration but immediately elevated to 1.4 times the basal expression until 12 hrs and continued up to 48 hrs **(Fig. 2A, B)**. The ALP area/TV and ALP-immunolocalization increased around 12 and 24 hrs, respectively; however, they did not show a significant difference at 24 hrs compared to the specimens at 0 hr **(Fig. 2C-J)**. In semithin sections and TEM images, preosteoblasts appeared to extend their cytoplasmic processes, with a relatively thickened preosteoblastic cell layer intervening between mature osteoblasts and blood vessels **(Fig. 2K-N)**. The *Sost* gene encoding sclerostin was significantly down-regulated from 1.5 hrs until 24 hrs **(Fig. 2O)**. Consistently, the number of sclerostin-positive osteocytes was attenuated from 1.5 to 12 hrs, though there was no significant reduction in *Sost* expression after 24 hrs compared to 0 hr **(Fig. 2O)**. Thus, osteoblastic cells, including preosteoblasts, were activated at the early stage of PTH action. As shown in previous studies [3, 4], we presumed that the synthesis of osteocyte-derived sclerostin is possibly blocked to activate osteoblastic cells.

Regarding catabolic markers, *Rankl* expression increased approximately sevenfold at 1.5 hrs but then returned to normal levels **(Fig. 3A-C)**. In contrast, the *Opg* level was transiently reduced at 1.5 hrs but then increased at 6 hrs. These findings strongly suggest that osteoclastogenesis and osteoclast activation are induced during the early stage of PTH administration but do not continue for an extended period. Indeed, the TRAP enzyme histochemistry and the number of TRAP-positive osteoclasts did not change **(Fig. 3D-K)**. A previous study described that a single subcutaneous injection of PTH [1-38] in rats promoted a transient increase in *Rankl* mRNA levels and decreased *Opg* levels [9], which could lead to transient osteoclast activation. Li *et al.* have shown significant upregulation of genes that stimulate osteoclastogenesis after anabolic PTH treatment, suggesting that transient osteoclast generation may be necessary for PTH-induced bone anabolism [10]. Therefore, during the early stage of PTH administration, molecules that activate osteoclastic differentiation and bone resorption are immediately elevated and quickly reduced afterward.

4. Conclusion

Intermittent administration of PTH, which induces a sudden but transient elevation of catabolic molecules and long-lasting elevation of anabolic molecules, may promote predominant anabolism.

Ethical approval

The study followed the principles for animal care and research use set by Hokkaido University.

Fundings

This study was partially supported by the Grants-in-Aid for Scientific Research of Japan Society for the Promotion of Science (JSPS, 19K10040, 22K09911 to Hasegawa T, 22K17000 to Yamamoto T, and 22K21006 to Maruoka H).

CRediT authorship contribution statement

Yamamoto T and **Maruoka H** are the main researchers who equally contributed to this work, including immunohistochemistry, gene expression, and TEM observation experiments. **Hasegawa T** is the chief of this research project, who organized collaborators and provided the complete outline of this study. **Hongo H**, **Yoshino H**, **Haraguchi-Kitakamae M**, **Liu X,** and **Yao Q** contributed to the experimental work, including the preparation of paraffin samples and statistical analyses. **Li M** and **Amizuka N** participated in the discussion and preparation of the manuscript. All authors have read and approved the final manuscript.

Declaration of competing interest

None of the authors declares a conflict of interest.

References

[1] Dempster DW, Zhou H, Recker RR, Brown JP, C Recknor CP, Lewiecki EM, et al. Remodeling- and modeling-based bone formation with teriparatide versus denosumab: A longitudinal analysis from baseline to 3 months in the AVA study. J Bone Miner Res 2018; 33(2):298-306.

[2] Yamamoto T, Hasegawa T, Sasaki M, Hongo H, Tsuboi K, Shimizu T, et al. Frequency of teriparatide administration affects the histological pattern of bone formation in young adult male mice. Endocrinology 2016; 157(7):2604-2620.

[3] Bellido T, Ali AA, Gubrij I, Plotkin LI, Fu Q, O'Brien CA, et al. Chronic elevation of parathyroid hormone in mice reduces expression of sclerostin by osteocytes: a novel mechanism for

hormonal control of osteoblastogenesis. Endocrinology 146(11):4577-4583, 2005.

[4] O'Brien CA, Plotkin LI, Galli C, Goellner JJ, Gortazar AR, Allen MR, et al. Control of bone mass and remodeling by PTH receptor signaling in osteocytes. PLoS One 2008; 3(8):e2942.

[5] Hasegawa T, Miyamoto-Takasaki Y, Abe M, Qiu Z, Yamamoto T, Yoshida T, et al. Histochemical examination on principal collagen fibers in periodontal ligaments of ascorbic acid-deficient ODS-od/od rats. Microscopy (Oxf) 2019; 68(5):349-358.

[6] Hasegawa T, Yamamoto T, Sakai S, Miyamoto Y, Hongo H, Qiu Z, et al. Histological effects of the combined administration of eldecalcitol and a parathyroid hormone in the metaphyseal trabeculae of ovariectomized rats. J Histochem Cytochem 2019; 67(3):169-184.

[7] Oda K, Amaya Y, Fukushi-Irié M, Kinameri Y, Ohsuye K, Kubota I, et al. A general method for rapid purification of soluble versions of glycosylphosphatidylinositol-anchored proteins expressed in insect cells: an application for human tissue-nonspecific alkaline phosphatase. J Biochem 1999; 126(4):694-699.

[8] Hasegawa T, Tokunaga S, Yamamoto T, Sakai M, Hongo H, Kawata T, et al. Evocalcet rescues secondary hyperparathyroidism-driven cortical porosity in CKD male rats. Endocrinology 2023; 164(4):bqad022.

[9] Onyia JE, Miles RR, Yang X, Halladay DL, Hale J, Glasebrook A, et al. In vivo demonstration that human parathyroid hormone 1-38 inhibits the expression of osteoprotegerin in bone with the kinetics of an immediate early gene. J Bone Miner Res. 2000; 15(5):863-871.

[10] Li X, Liu H, Qin L, Tamasi J, Bergenstock M, Shapses S, et al. Determination of dual effects of parathyroid hormone on skeletal gene expression in vivo by microarray and network analysis. J Biol Chem 2007; 282(45): 33086-33097.

Figure Legends

Figure 1.

Histological and histomorphometric changes of femora after a single injection of PTH

Panels **A-G** show low-magnified histological images after PTH administration, and panels **H-N** demonstrate highly magnified images of metaphyses corresponding to panels **A-G**. No histological differences are observed after PTH administration. Panels **O-R** present static parameters of bone histomorphometry. There are no significant differences in the values of BV/TV, Tb.Th., Tb.N., and Tb.Sp during the experiments (0, 1.5, 3, 6, 12, 24, and 48 hrs). Panels **S** and **T** display the serum concentration of Ca and Pi, respectively. There is a slight tendency for a rapid and transient increase in serum Ca at 1.5 hrs after the PTH injection, although it is not statistically significant.

Bars, A-G:100μm, H-N:200μm

Figure 2.

The expression of *Runx2* and *Sost* and histological changes of osteoblastic cells

Panels **A** and **B** show RT-PCR and a graph of real-time PCR representing the chronological change of *Runx2* expression. Note the sudden and significant decrease in *Runx2* expression at 1.5 hrs, followed by an immediate elevation to 1.4 times the normal level until 12 hrs, continuing up to 48 hrs after the PTH injection. Panel **C** shows the chronological changes in ALP positive areas/TV, while panels **D-J** display ALP immunolocalization (brown color) in the metaphysis during the experiments. Semithin sections **(K, M)** and TEM images **(L, N)** demonstrate preosteoblasts extending their cytoplasmic processes intervening blood vessels and mature osteoblasts after 24 hrs **(M, N)** compared to 0 hr **(K, L)**. Panels **O** and **P** present the chronological change of *Sost* expression assessed by real-time PCR **(O)** and the ratios of sclerostin-positive osteocytes **(P)**. The immediate reduction of *Sost* gene expression from 1.5 hrs, with a significant decrease until 24 hrs **(O)** can be noted. Consistently, the ratio of sclerostin-positive osteocytes significantly decreased from 1.5 to 12 hrs, though there is no significant reduction in *Sost* expression after 48 hrs **(P)**.

Bars, D-J: 200μm, K and M: 10μm, L and N: 5μm

Figure 3.

The expression profile of *Rankl* and histological changes of TRAP-positive osteoclasts

Panels **A** and **B** show the gene expression of *Rankl* and *Osteoprotegerin (Opg)* assessed by RT-PCR, respectively. Graph **C** demonstrates the chronological changes in *Rankl* and *Opg* mRNA levels during the experiments. *Rankl* expression immediately increased approximately sevenfold at 1.5 hrs but then returned to normal levels. On the other hand, *Opg* is transiently reduced at 1.5 hrs and then increased

at 6 hrs. The number of TRAP-positive osteoclasts does not statistically change, as seen in the distribution **(D-J)** and statistical analysis **(K)** of the number of TRAP-positive osteoclasts.

Bars, D-J: 200μm

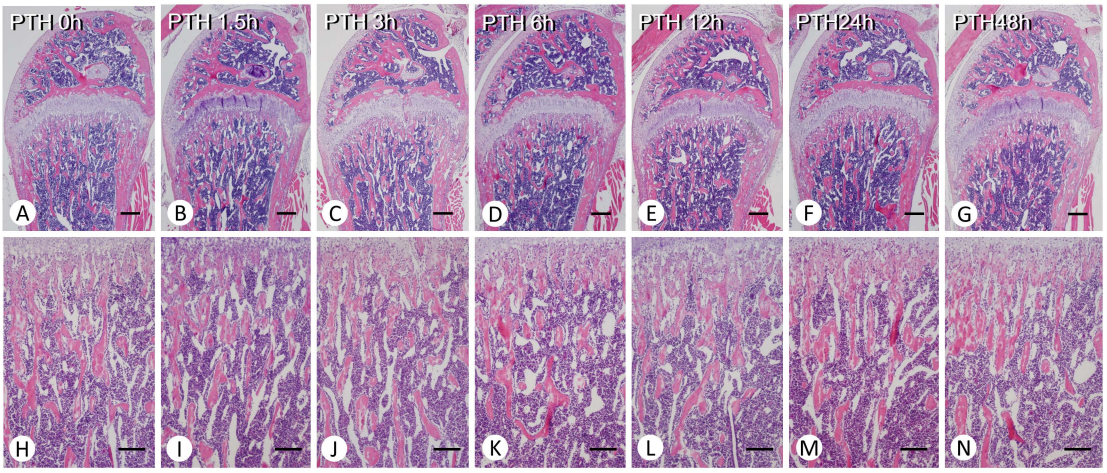
PTH 0h
PTH 1.5h
PTH 3h
PTH 6h
PTH 12h
PTH24h
PTH48h
A
B
C
D
E
F
G
H
I
J
K
L
M
N

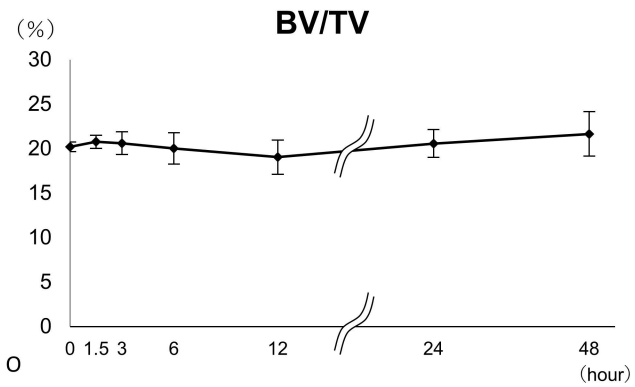
BV/TV
(%)
30
25
20
15
10
5
0
0 1.5 3 6 12 24 48
(hour)
O

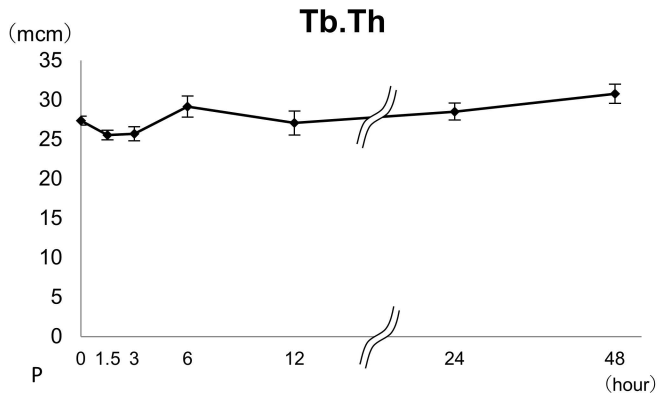
Tb.Th
(mcm)
35
30
25
20
15
10
5
0
0 1.5 3 6 12 24 48
(hour)
P

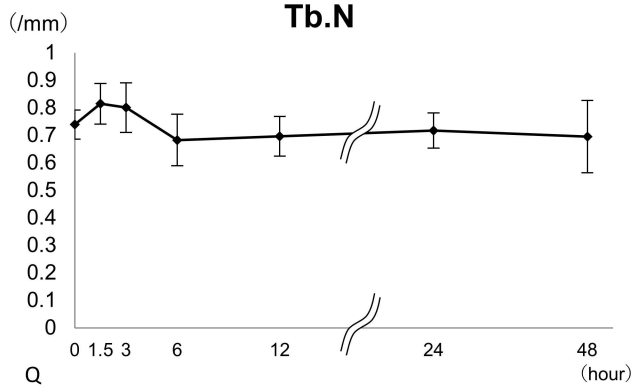
Tb.N
(/mm)
1
0.9
0.8
0.7
0.6
0.5
0.4
0.3
0.2
0.1
0
0 1.5 3 6 12 24 48
(hour)
Q

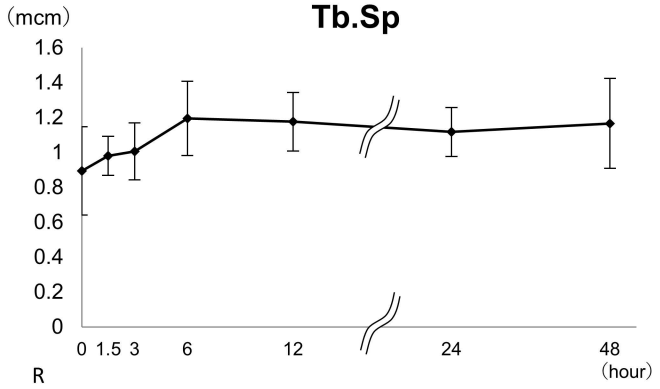
Tb.Sp
(mcm)
1.6
1.4
1.2
1
0.8
0.6
0.4
0.2
0
0 1.5 3 6 12 24 48
(hour)
R

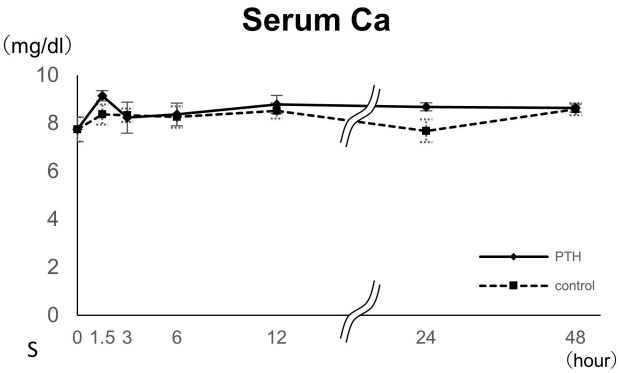
Serum Ca
(mg/dl)
10
8
6
4
2
0
PTH
control
0 1.5 3 6 12 24 48
(hour)
S

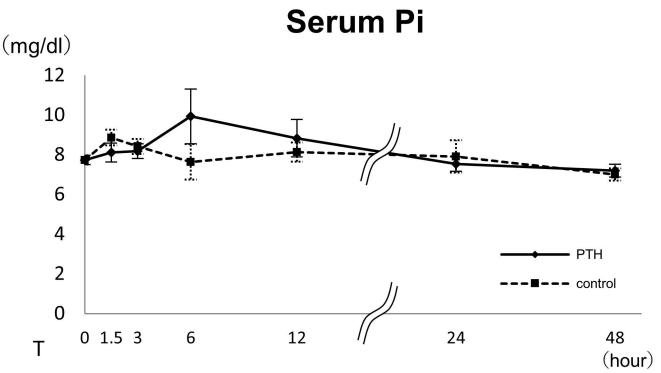
Serum Pi
(mg/dl)
12
10
8
6
4
2
0
PTH
control
0 1.5 3 6 12 24 48
(hour)
T

Fig. 1

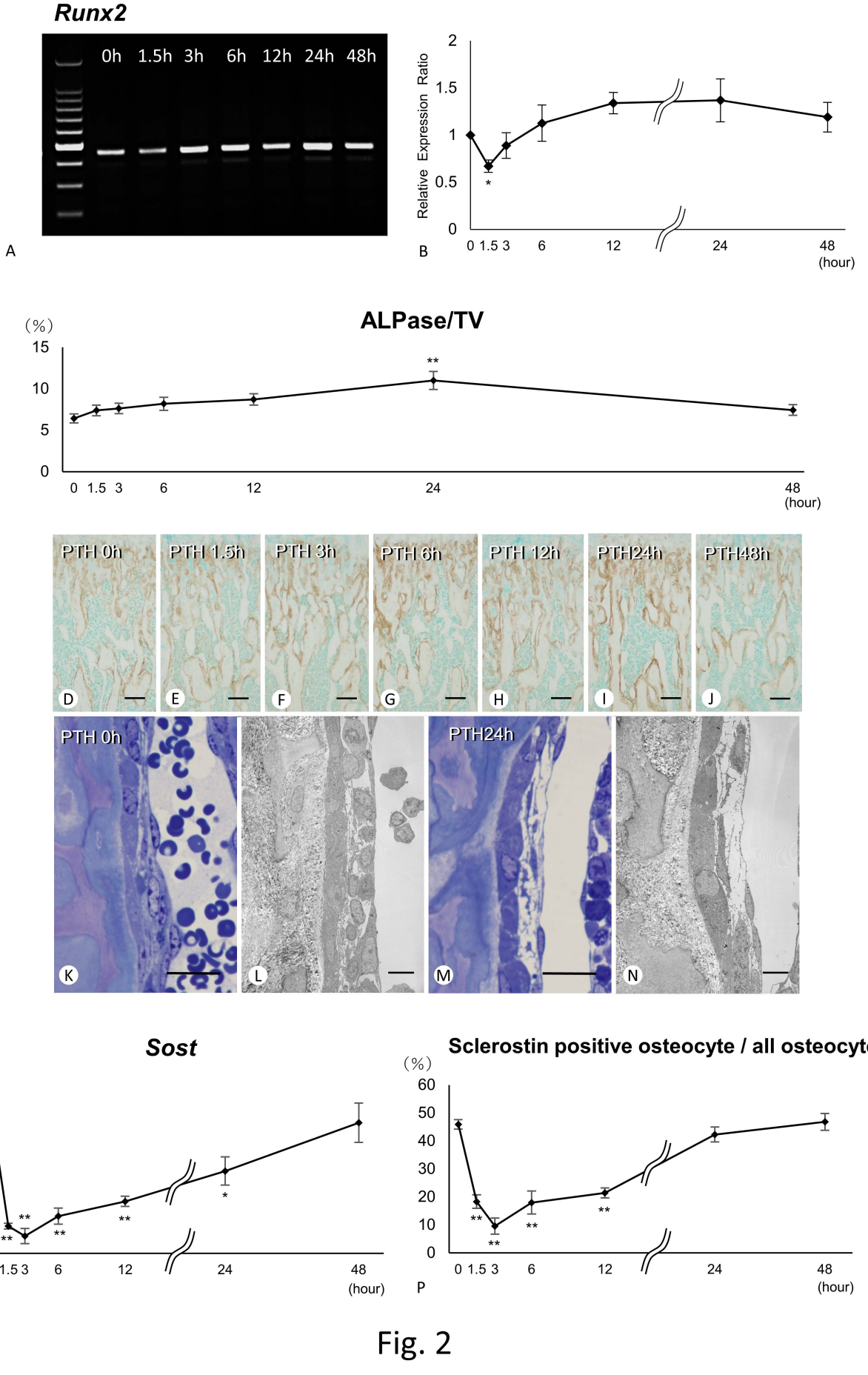
Runx2
0h 1.5h 3h 6h 12h 24h 48h
A
Relative Expression Ratio
2
1.5
1
0.5
0
*
0 1.5 3 6 12 24 48
(hour)
B
ALPase/TV
(%)
15
10
5
0
**
0 1.5 3 6 12 24 48
(hour)
PTH 0h
PTH 1.5h
PTH 3h
PTH 6h
PTH 12h
PTH24h
PTH48h
D
E
F
G
H
I
J
PTH 0h
PTH24h
K
L
M
N
Sost
Relative Expression Ratio
1.2
1
0.8
0.6
0.4
0.2
0
0 1.5 3 6 12 24 48
(hour)
O
Sclerostin positive osteocyte / all osteocyte
(%)
60
50
40
30
20
10
0
0 1.5 3 6 12 24 48
(hour)
P

Fig. 2

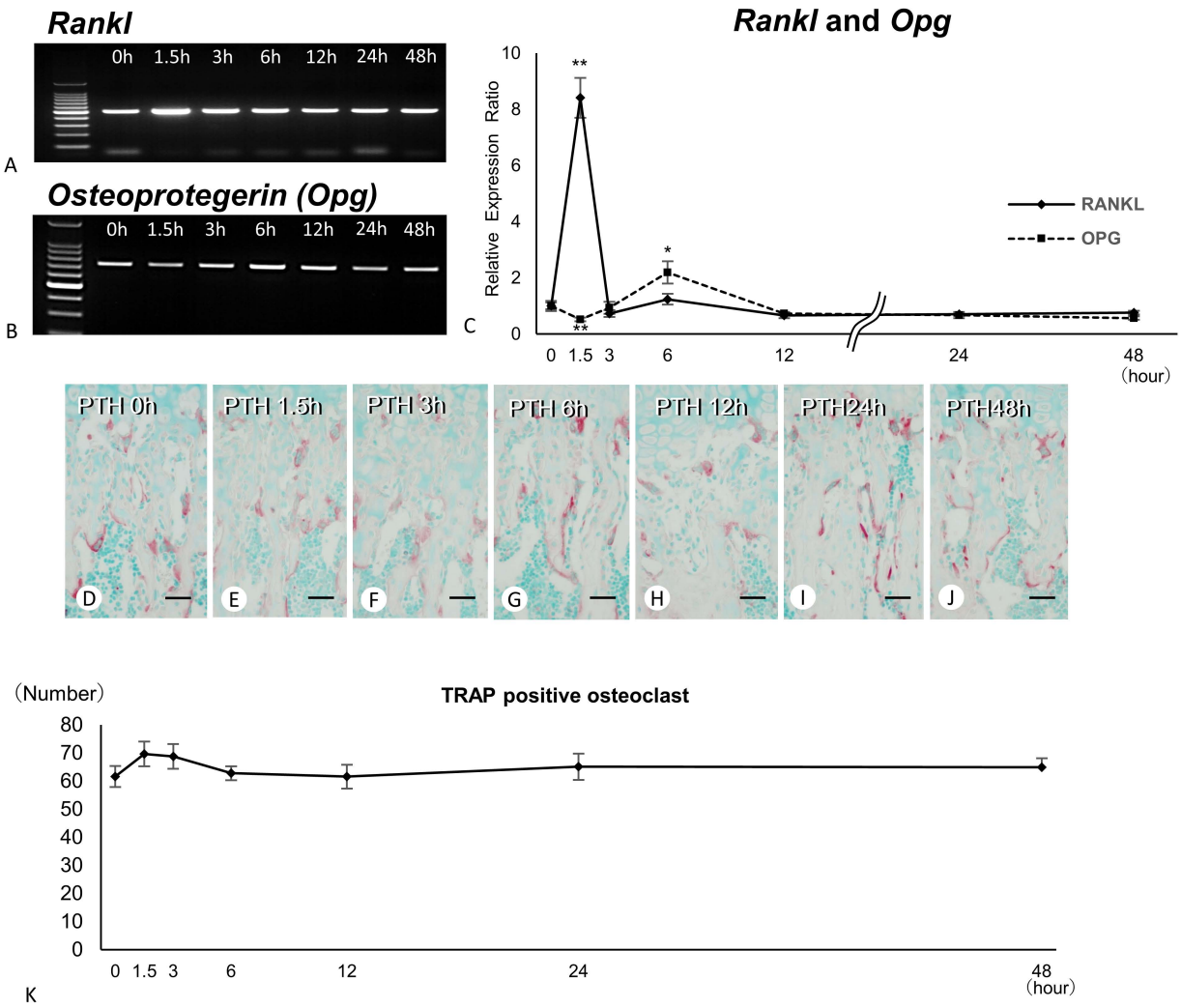
Rankl
0h 1.5h 3h 6h 12h 24h 48h
A
Osteoprotegerin (Opg)
0h 1.5h 3h 6h 12h 24h 48h
B
Rankl and Opg
Relative Expression Ratio
RANKL
OPG
C
0 1.5 3 6 12 24 48
(hour)
PTH 0h
PTH 1.5h
PTH 3h
PTH 6h
PTH 12h
PTH24h
PTH48h
D
E
F
G
H
I
J
(Number)
TRAP positive osteoclast
0 1.5 3 6 12 24 48
(hour)
K

Fig. 3